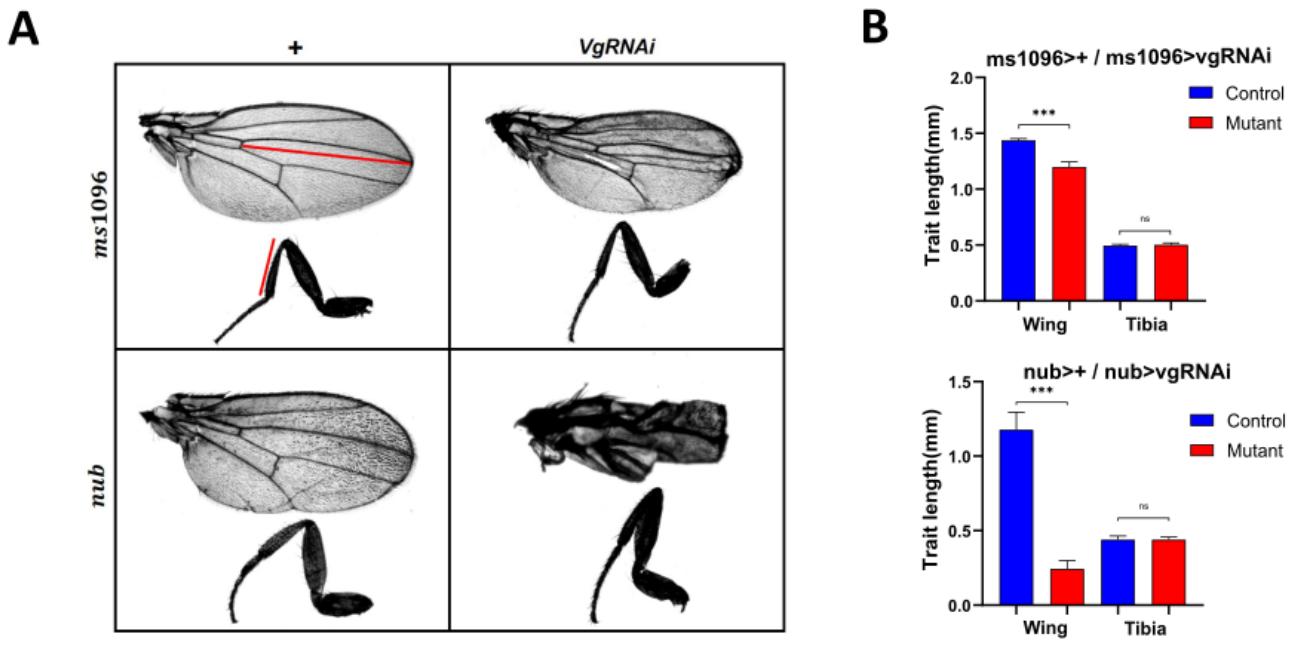

Fig. S1. Legs are not affected by changes in *vg* expression (A) Wing and tibia phenotypes of *D. melanogaster* flies expressing a vgRNAi under the control of ms1096Gal4 or nubGal4 compared to the corresponding controls (ms1096>+ or nub>+, respectively). P/D lengths in wings and tibias were taken to determine wing/tibia scaling relationships in Fig. 2, S2, 4, S4 (red lines). (B) Quantification of tibia and wing P/D lengths of the genotypes shown in A. Mutants (red bars) correspond to the vgRNAi-expressing flies. Statistical comparisons correspond to Student t-tests. ***=*p-value<0.001, ns* = not statistically significant (*p-value>0.05*). ms1096>vgRNAi, *n*= 13; ms1096>+, *n*= 10; nub>vgRNAi, *n*= 9; nub>+, *n*= 7.

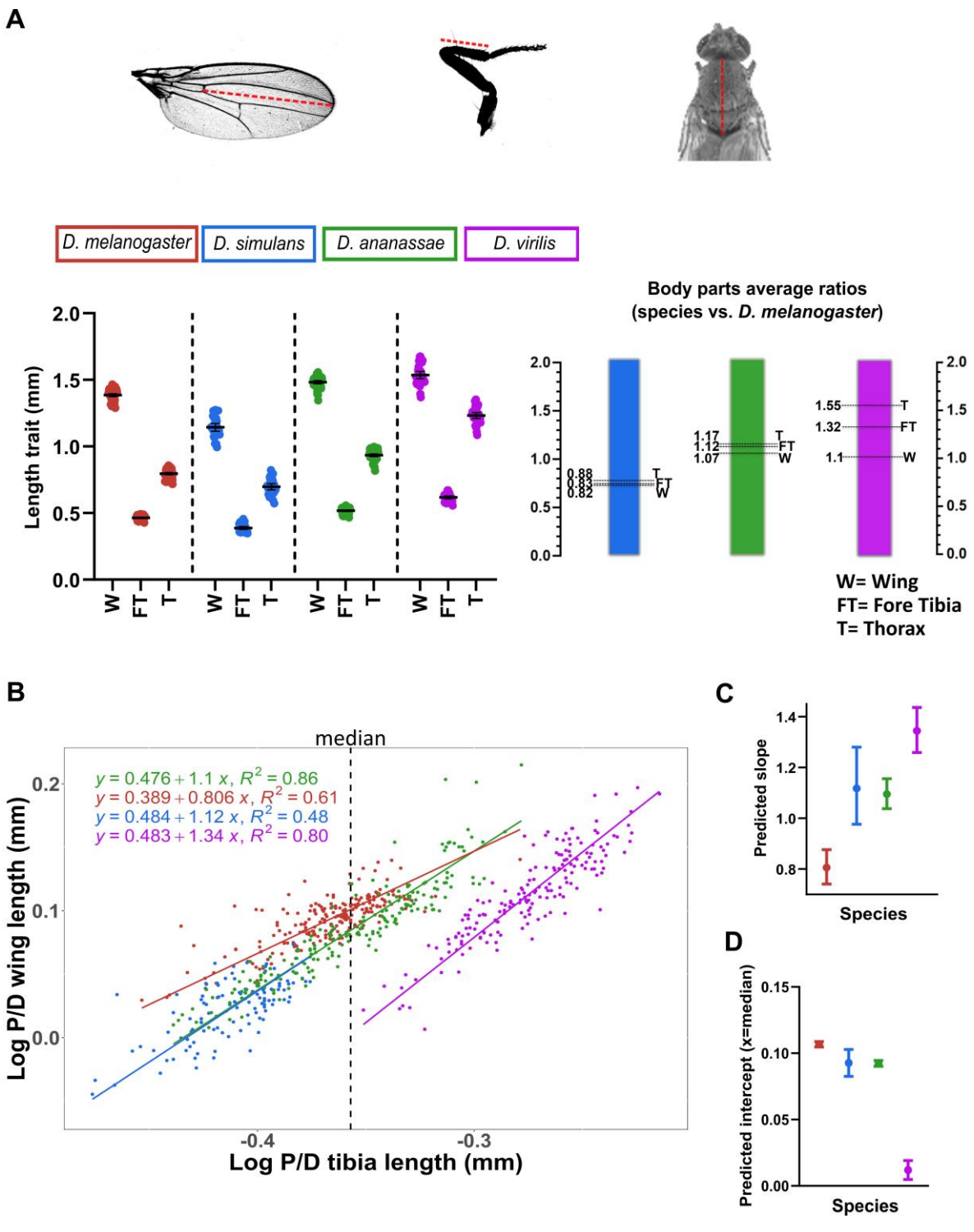

Fig. S2. Wing-to-tibia scaling relationships reveal a reduction of wing size in *D. virilis* males. (A) P/D trait measures in *Drosophila* species. Average length of left/right wings and fore tibias, as well as thorax measures are represented for each male flies. Right panel shows the body parts average ratios (species vs. *D. melanogaster*) for each measured trait. *D. melanogaster n*= 60, *D. simulans n*=30, *D. ananassae n*=58, *D. virilis n*=34. (B) Wing-to-tibia static scaling relationships fitted using model II of regression (SMA) in male *Drosophila*. Red, blue, green and purple dots correspond to *D. melanogaster, D. simulans, D. ananassae* and *D. virilis* respectively. (C) Predicted slope of wing-tibia scaling relationship for each *Drosophila* species. (D) Predicted intercept of wing-tibia scaling relationship for each *Drosophila* species. The predicted intercept value was obtained through SMA adjusted to the median log(tibia) of all species (dotted line in panel B). Error bars are 95% confidence intervals. The experiment was replicated two times in the laboratory. *D. melanogaster, n*=215; *D. simulans, n*=112; *D. ananassae, n*=195; *D. virilis, n*=179. T=thorax; FT=fore tibia; W=wing.

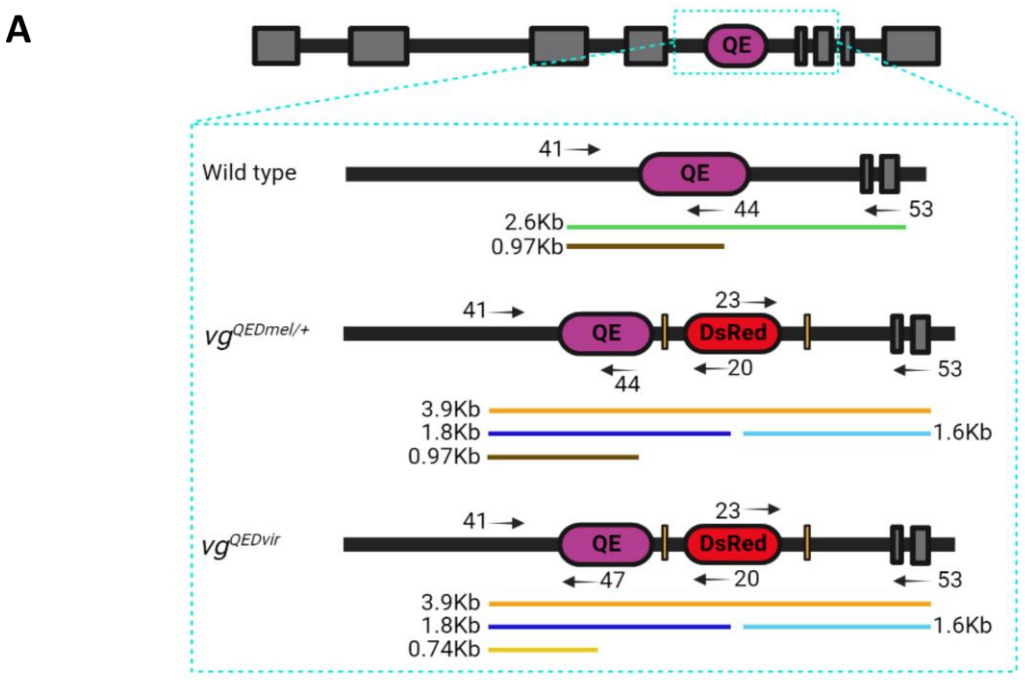

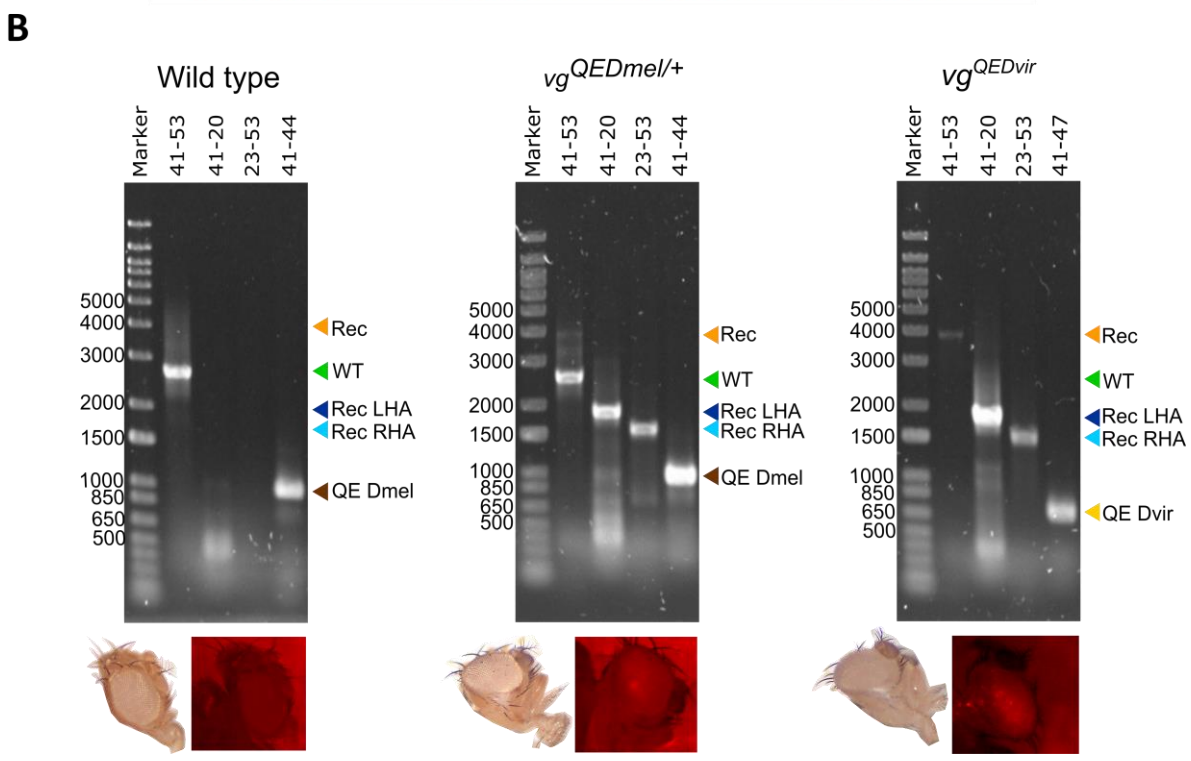

Fig. S3. Molecular confirmation of the *vg*^{QE} replacement. (A) Size of amplification products used for the identification of the *vg*^{QE} replacement are shown in the colored lines. Primers and the sense that were used are indicated with black arrows. (B) Amplification products in wild type, *vg*^{QEDmel}/+, and *vg*^{QEDvir}/*vg*^{QEDvir} flies. We used oligos 41 and 53 (see Table S1) for the evaluation of the Recombinant (Rec) and/or the wild-type (WT) product; oligos 41 and 20 (see Table S1) were used for the identification of the Recombinant Left homologous Arm (Rec-LHA); oligos 23 and 53 (see Table S1) were used for the amplification of the Recombinant Right Homologous Arm (RecRHA); *vg*^{QEDmel}/+, and *vg*^{QEDvir}/*vg*^{QEDvir} were evaluated with oligos 41 and, 44 or 47 (see Table S1), respectively. At the bottom panels, evidence of fluorescent eyes is shown as a confirmation that the DsRed marker is present.

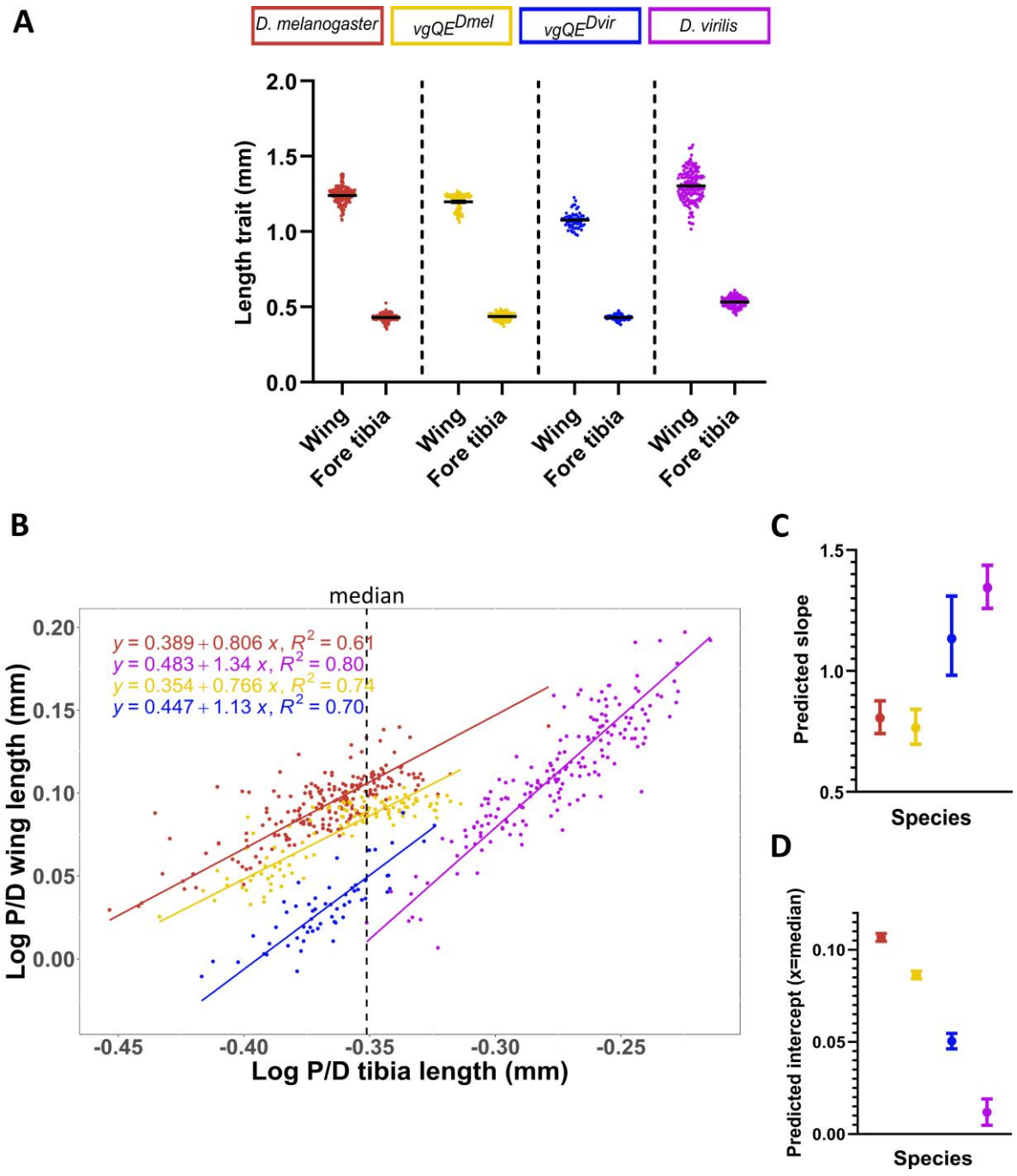

Fig. S4. *D. virilis vg*^{QE} replacement into *D. melanogaster* results in allometric changes in males. (A) Proximal-distal trait measures in *Drosophila* species (*D. melanogaster, D.virilis)* and CRISPR/Cas9 mutants (*vg*^{QEDmel}, *vg*^{QEDvir}). Average length of left/right wings and fore tibias are represented for each male flies. (B) Wing-to-tibia static static relationships fitted using model II of regression (SMA).

Yellow and blue lines and dots correspond to HDR replacements using *vg*^{QEDmel} and *vg*^{QEDvir} respectively. Red and purple lines and dots show the scaling relationship in *D. melanogaster* and *D. virilis* wild type animals respectively. (C) Predicted slope of wing-tibia scaling relationship for *D. melanogaster, D. virilis,* and the CRISPR/Cas9 edited stocks. (D) Predicted intercept of wing-tibia scaling relationship for *D. melanogaster, D. virilis,* and the CRISPR/Cas9 edited stocks. The predicted intercept value was obtained through SMA adjusted to the overall median log(tibia size) of *D. melanogaster*, *D. virilis* and CRISPR/Cas9 stocks (dotted line in panel B). Error bars are 95% confidence intervals. *D. melanogaster, n*= 215; *vg*^{QEDmel}, *n*=118; *vg*^{QEDvir}, *n*=59' *D. virilis, n*=179.

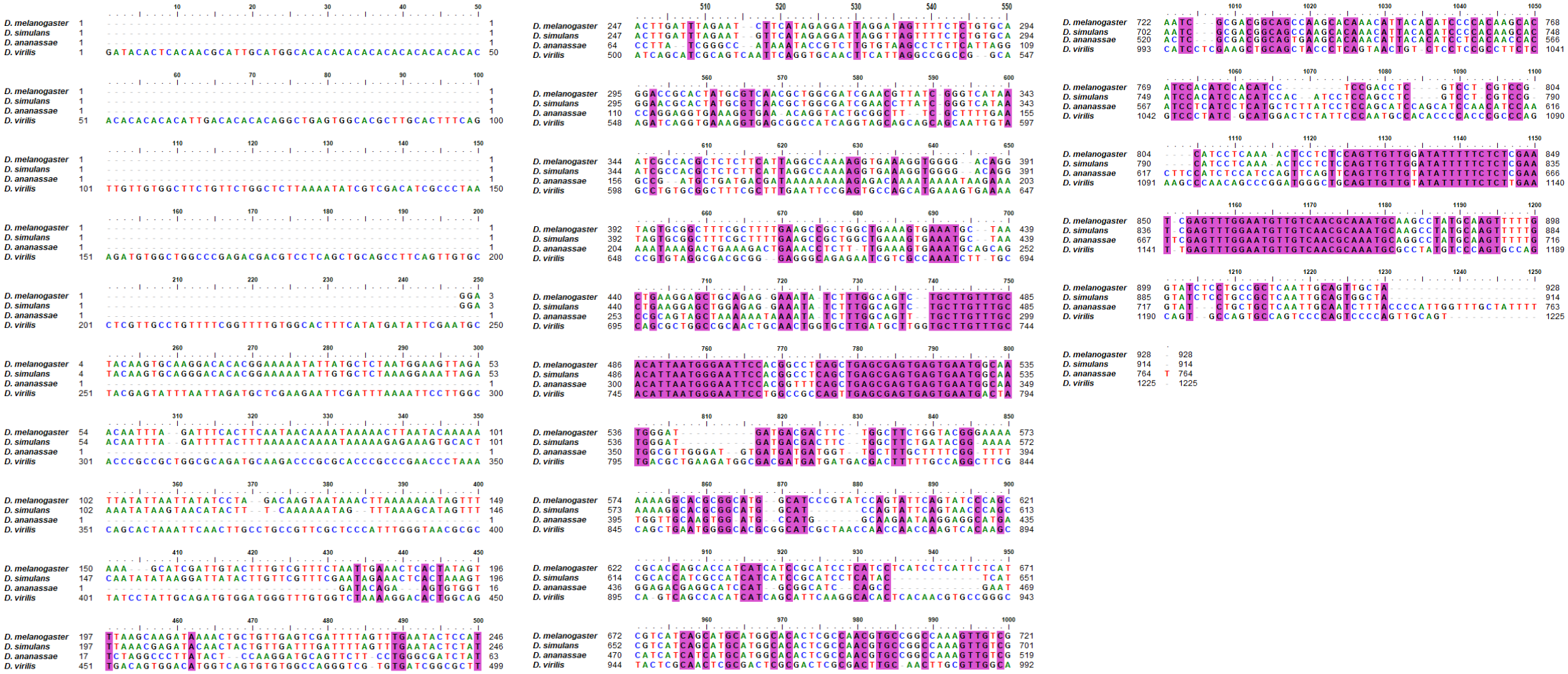

Fig. S5. Multiple alignment of QE sequences in *Drosophila* species. Sequences obtained from local alignments using the Smith–Waterman algorithm were processed in Clustal Omega for multiple alignment. Conserved bases in the four species are highlighted in pink.

Table S1. Oligonucleotides

N°	Oligo name	Sequence
2	QE3’	GCTATTTCTAGCTCTAAAACTTATGTGTAATGGAGCTCCCGACGTTAAATTGAAAATAGGTC
3	TEA2	GGAAAGATATCCGGGTGAACTTCGCAGTATGGTGATTCGATTCGTTTTAGAGCTAGAAATAGCAAG
20	mCherry-R	CTTGGTCACCTTCAGCTTGG
23	DsRed1C Forward	GGACATCACCTCCCACAACG
41	RecDsp F	GCCGCATAGATTCCTCATTACG
44	QE sp R	CATTCACTCACTCGCTCAGCTG
47	QE vir R	GATTTGGCGACGATTCTCTGC
53	Outside_screening_R	CGATCGGGCGATCGACTCAC
352	M13 Forward	TGTAAAACGACGGCCAGT
596	pCFD4 upstream seq	TAGTCCCATCATTGGCATGGTAGGTACCCG
835	pBR322 fwd	CAGCTCGAGGCTCTTCCGTCAATCG
836	pBR322 rev	CTAGCATGCAAGAATTCCACCTGC
837	DsRed fwd	CGGCCGCGGACATATGCACACCTG
838	DsRed rev	TGGAGATCTTTACTAGTGCTCTTC
839	DmLHA2/pBR322 fwd	GTGGAATTCTTGCATGCTAGGCCACTCGCTTGTTCTTTCGATTTC
840	DmLHA2/DsRed rev	TGTGCATATGTCCGCGGCCGTCGAATCACCATACTGCATTTGGTG
841	DmRHA1/DsRed fwd	AGCACTAGTAAAGATCTCCATAATGGAGATGTCTTGCTCCCGGC
842	DmRHA1/pBR322 rev	GACGGAAGAGCCTCGAGCTGCCTACAAGCAGATATCCGATTGG
843	DmLHA2 rev	TCGAATCACCATACTGCATTTGGTG
844	Dmel/virQE fwd	AATGCAGTATGGTGATTCGACTAGTTGGAATGTGCTAT
845	DmelQE rev	TGTGCATATGTCCGCGGCCGTGTGTAATGGAGCTCCC
846	DvirQE rev	TGTGCATATGTCCGCGGCCGAGTGTAATGGAGCTCTG